



A molecular framework for the control of adventitious rooting by TIR1/AFB2-Aux/IAA-dependent auxin signaling in Arabidopsis

Abdellah Lakehal, Salma Chaabouni, Emilie Cavel, Rozenn Le Hir, Alok Ranjan, Zahra Raneshan, Ondrej Novák, Daniel Pacurar, Irene Perrone, François Jobert, et al.

► To cite this version:

Abdellah Lakehal, Salma Chaabouni, Emilie Cavel, Rozenn Le Hir, Alok Ranjan, et al.. A molecular framework for the control of adventitious rooting by TIR1/AFB2-Aux/IAA-dependent auxin signaling in Arabidopsis. *Molecular Plant*, 2019, 12 (11), pp.1499-1514. 10.1016/j.molp.2019.09.001 . hal-02621817

HAL Id: hal-02621817

<https://hal.inrae.fr/hal-02621817>

Submitted on 20 Jul 2022

HAL is a multi-disciplinary open access archive for the deposit and dissemination of scientific research documents, whether they are published or not. The documents may come from teaching and research institutions in France or abroad, or from public or private research centers.

L'archive ouverte pluridisciplinaire **HAL**, est destinée au dépôt et à la diffusion de documents scientifiques de niveau recherche, publiés ou non, émanant des établissements d'enseignement et de recherche français ou étrangers, des laboratoires publics ou privés.



Distributed under a Creative Commons Attribution - NonCommercial 4.0 International License

A Molecular Framework for the Control of Adventitious Rooting by the TIR1/AFB2-Aux/IAA-Dependent Auxin Signaling in Arabidopsis

Abdellah Lakehal^{1#}, Salma Chaabouni^{1#}, Emilie Cavel^{1,a}, Rozenn Le Hir², Alok Ranjan¹, Zahra Raneshan^{1,3}, Ondřej Novák^{4,5}, Daniel I. Păcurar¹, Irene Perrone^{1,b}, François Jobert^{6,c}, Laurent Gutierrez⁶, Laszlo Bakó¹ and Catherine Bellini^{1,2 *}

¹ Umeå Plant Science Centre, Department of Plant Physiology, Umeå University, SE-90736 Umeå, Sweden

² Institut Jean-Pierre Bourgin, INRA, AgroParisTech, CNRS, Université Paris-Saclay, 78000 Versailles, France

³ Department of Biology, Faculty of Science, Shahid Bahonar University, Kerman, Iran

⁴ Laboratory of Growth Regulators, Faculty of Science, Palacký University and Institute of Experimental Botany, The Czech Academy of Sciences, 78371 Olomouc, Czech Republic

⁵ Umeå Plant Science Centre, Department of Forest Genetics and Physiology, Swedish Agriculture University, SE-90183 Umeå, Sweden

⁶ Centre de Ressources Régionales en Biologie Moléculaire (CRRBM), Université de Picardie Jules Verne, 80039 Amiens, France

These two authors equally contributed to the work.

^a Present address: Centre de Ressources Régionales en Biologie Moléculaire (CRRBM), Université de Picardie Jules Verne, 80039 Amiens, France

^b Present address: Institute for Sustainable Plant Protection, National Research Council of Italy, Turin, Italy

^c Present address: Umeå Plant Science Centre, Department of Forest Genetics and Plant Physiology, SLU, SE-90736 Umeå, Sweden

* To whom correspondence should be addressed:

Pr Catherine Bellini (Catherine.Bellini@umu.se /Catherine.Bellini@inra.fr)

Umeå Plant Science Centre, Department of Plant Physiology,

Umeå University, SE-90736 Umeå, Sweden

Phone: +46907869624

Short title: TIR1/AFBs, AuxIAAs and adventitious rooting

SHORT SUMMARY

Auxin mediates plethora of developmental programs. We provide evidence on how the canonical auxin-sensing machinery functions to control the JA pool during adventitious rooting. We show that TIR1, besides its function in negatively regulating JA biosynthesis, acts with AFB2 and IAA6, IAA9 and IAA17 to form a sensing module regulating the expression of the JA conjugating enzymes GH3.3, GH3.5 and GH3.6.

ABSTRACT

In *Arabidopsis thaliana*, canonical auxin-dependent gene regulation is mediated by 23 transcription factors from the AUXIN RESPONSE FACTOR (ARF) family interacting with 29 auxin/indole acetic acid repressors (Aux/IAA), themselves forming coreceptor complexes with one of six TRANSPORT INHIBITOR1/AUXIN-SIGNALING F-BOX (TIR1/AFB) PROTEINS. Different combinations of co-receptors drive specific sensing outputs, allowing auxin to control a myriad of processes. Considerable efforts have been made to discern the specificity of auxin action. However, owing to a lack of obvious phenotype in single loss-of-function mutants in *Aux/IAA* genes, most genetic studies have relied on gain-of-function mutants, which are highly pleiotropic. *ARF6* and *ARF8* are positive regulators of adventitious root initiation upstream of jasmonate, but the exact auxin co-receptor complexes controlling the transcriptional activity of these proteins was still unknown. Here using loss-of-function mutants we show that *IAA6*, *IAA9* and *IAA17* genes act additively in the control of AR initiation, and by performing protein-protein interaction analysis, we show that the corresponding proteins interact with ARF6 and/or ARF8 and likely repress their activity. We also demonstrate that *TIR1* and *AFB2* are positive regulators of adventitious root formation and suggest a dual role for TIR1 in the control of JA biosynthesis and conjugation, as revealed by upregulation of several JA biosynthesis genes in the *tir1-1* mutant. We propose that in the presence of auxin, TIR1 and AFB2 form specific sensing complexes with IAA6, IAA9 and/or IAA17 that modulate JA homeostasis to control AR initiation.

Key words: TIR1/AFB, AuxIAA, jasmonate, adventitious roots, Arabidopsis

INTRODUCTION

In *Arabidopsis thaliana*, auxin-dependent gene regulation is mediated by the 23 members of the AUXIN RESPONSE FACTOR (ARF) family of transcription factors, which can either activate or repress transcription (Okushima et al., 2005; reviewed in Chapman and Estelle, 2009 and Guilfoyle and Hagen, 2007). Interaction studies have shown that most of the auxin/indole-3-acetic acid (Aux/IAA) inducible proteins can interact with ARF activators (reviewed in Guilfoyle and Hagen, 2007; Vernoux et al., 2011). Aux/IAAs mediate recruitment of the TOPLESS corepressor (Szemenyei et al., 2008) and act as repressors of transcription of auxin-responsive genes. When the auxin level rises, it triggers interaction of the two components of the auxin co-receptor complex, an F-box protein from the TRANSPORT INHIBITOR1/AUXIN-SIGNALING F-BOX PROTEIN (TIR1/AFB) family (Kepinski and Leyser 2005; Dharmasiri, et al. 2005a) and an Aux/IAA protein, promoting ubiquitination and 26S-mediated degradation of the latter (Gray et al., 2001). Degradation of the Aux/IAA protein releases the ARF activity and subsequent activation of the auxin-responsive genes (reviewed in Wang and Estelle, 2014; Weijers and Wagner, 2016). TIR1/AFBs show different affinities for the same Aux/IAA (Calderon Villalobos et al., 2012; Parry et al., 2009), suggesting that different combinations of TIR1/AFB receptors may partially account for the diversity of auxin response. In addition, it has been shown that most Aux/IAAs can interact with many Aux/IAAs and ARFs in a combinatorial manner, increasing the diversity of possible auxin signaling pathways that control many aspects of plant development and physiology (Boer et al., 2014; reviewed in Guilfoyle and Hagen, 2012; Korasick et al., 2014; Nanao et al., 2014; Vernoux et al., 2011; Weijers et al., 2005). Several studies have suggested specialized functions for some of the ARF and IAA combinations during embryo development (Hamann et al., 2002), lateral root (LR) development (De Rybel et al., 2010; De Smet et al., 2010; Fukaki et al., 2002; Lavenus et al., 2013; Tatematsu et al., 2004), phototropism (Sun et al., 2013) and fruit development (Wang et al., 2005). However, most of these studies involved characterization of gain-of-function stabilizing mutations, which limited identification of more specialized functions for individual Aux/IAA genes. To date, genetic investigations of Aux/IAA genes have been hampered by the lack of obvious phenotype in the loss-of-function mutants (Overvoorde et al., 2005). Nevertheless, recent careful characterization of a few of the mutants identified more precise functions in primary or LR development for *IAA3* or *IAA8* (Arase et al., 2012; Dello Ioio et al., 2008) or in the response to environmental stresses for *IAA3*, *IAA5*, *IAA6* and *IAA19* (Orosa-Puente et al., 2018; Shani et al., 2017).

To decipher the role of auxin in the control of adventitious root (AR) development, which is a complex trait with high phenotypic plasticity (reviewed in Bellini et al., 2014 and Geiss et al., 2009), we previously identified a regulatory module composed of three *ARF* genes (two activators *ARF6* and *ARF8*, and one repressor *ARF17*) and their regulatory microRNAs (miR167 and miR160) (Gutierrez et al., 2009). These genes display overlapping expression domains, interact genetically and regulate each other's expression at transcriptional and post-transcriptional levels by modulating the availability of their regulatory microRNAs miR160 and miR167 (Gutierrez et al., 2009). The three ARFs control the expression of three auxin inducible *Gretchen Hagen 3 (GH3)* genes encoding acyl-acid-amido synthetases (GH3.3, GH3.5 and GH3.6) that, in addition to inactivating IAA (Staswick et al., 2005), inactivate jasmonic acid (JA), an inhibitor of AR initiation in *Arabidopsis* hypocotyls (Gutierrez et al., 2012; Supplemental Figure 1A). In a yeast two-hybrid system, ARF6 and ARF8 proteins were shown to interact with almost all Aux/IAA proteins (Vernoux et al., 2011). Therefore, we propose a model in which increased auxin levels facilitate formation of a coreceptor complex with at least one TIR1/AFB protein and subsequent degradation of Aux/IAs (Supplemental Figure 1B), thereby releasing the activity of ARF6 and ARF8 and the transcription of *GH3* genes. In the present work, we describe identification of members of the potential co-receptor complexes involved in this pathway. Using loss-of-function mutants, we demonstrate that *TIR1* and *AFB2* are positive regulators, whereas *IAA6*, *IAA9* and *IAA17* are negative regulators of AR formation. We suggest that TIR1 and AFB2 form co-receptor complexes with at least three Aux/IAA proteins (*IAA6*, *IAA9* and *IAA17*), which negatively control *GH3.3*, *GH3.5* and *GH3.6* expression by repressing the transcriptional activity of ARF6 and ARF8, thereby modulating JA homeostasis and consequent AR initiation. In addition, we show that several genes involved in JA biosynthesis are upregulated in the *tir1-1* mutant, suggesting a probable dual role of TIR1 in both the biosynthesis and conjugation of jasmonate.

RESULTS

TIR1 and AFB2 but not other AFB proteins control adventitious root initiation in *Arabidopsis* hypocotyls

To assess the potential contributions of different TIR/AFB proteins to regulation of adventitious rooting in *Arabidopsis*, we analyzed AR formation in *tir1-1*, *afb1-3*, *afb2-3*, *afb3-4*, *afb4-8*, *afb5-5* single knockout (KO) mutants, double and triple mutants using previously described conditions ((Gutierrez et al., 2009; Sorin et al., 2005) and Figure 1A).

The average number of ARs developed by *afb1-3*, *afb3-4*, *afb4-8*, *afb5-5* single mutants and *afb4-8afb5-5* double mutants did not differ significantly from the average number developed by wild-type seedlings (Figure 1A). These results suggest that AFB1, AFB3, AFB4 and AFB5 do not play a significant role in AR initiation. In contrast, *tir1-1* and *afb2-3* single mutants produced 50% fewer ARs than the wild-type plants and the *tir1-1afb2-3* double mutant produced even fewer, indicating an additive effect of the mutations (Figure 1A). The *afb1-3afb2-3* and *afb2-3afb3-4* double mutants retained the same phenotype as the *afb2-3* single mutant, and the triple mutant *tir1-1afb1-3and afb3-4* had the same phenotype as the *tir1-1* single mutant confirming a minor role, if any, of AFB1 and AFB3 in AR initiation. We also checked the root phenotype of the *tir1-1* and *afb2-3* single mutants and *tir1-1afb2-3* double mutant under the growth conditions used. No significant differences were observed in the primary root length (Supplemental Figure 2A), but the number of LRs was slightly but significantly decreased in both the *tir1-1* and *afb2-3* single mutants and dramatically decreased in the double mutant (Supplemental Figure 2B), as already shown by others (Dharmasiri et al., 2005b; Parry et al., 2009, Xuan et al., 2015). This resulted in a reduction of the LR density in all genotypes (Supplemental Figure 2C), confirming the additive and pleiotropic role of the TIR1 and AFB2 proteins. In order to confirm that the growth conditions we used to induce ARs did not compromise the root development compared to the canonical conditions used to study LR development, we performed similar experiments with seedlings grown in the light for ten days and obtained similar results (Supplemental Figure 2J-L)

TIR1 and AFB2 proteins are expressed in young seedlings during AR initiation

To analyze the expression pattern of the TIR1 and AFB2 proteins during the early stages of AR initiation and development, plants expressing the translational fusions *pTIR:cTIR1:GUS* or *pAFB2:cAFB2:GUS* were grown as previously described (Gutierrez et al., 2009). At time 0 (T0), i.e., in etiolated seedlings just before transfer to the light, the TIR1:GUS and AFB2:GUS proteins were strongly expressed in the root apical meristem, apical hook and cotyledons. Interestingly AFB2:GUS was also detected in the vascular system of the root and the hypocotyl, whereas TIR1:GUS was not detectable in those organs (Figure 1B). Nine hours after transfer to the light, TIR1:GUS protein disappeared from the cotyledons but was still strongly expressed in the shoot and root meristems. Its expression was increased slightly in the upper part of the hypocotyl. In contrast, AFB2:GUS was still highly detectable in the shoot and root meristems, cotyledons and vascular system of the root.

In addition, its expression was induced throughout almost the entire hypocotyl (Figure 1B). Seventy-two hours after transfer to the light, TIR1:GUS and AFB2:GUS showed almost the same expression pattern, which was reminiscent of that previously described in light grown seedlings (Parry et al., 2009). None of the proteins were detectable in the cotyledons. However, they were present in the shoot meristem and young leaves and the apical root meristem. In the hypocotyl and root, the TIR1:GUS and AFB2:GUS proteins were mainly detectable in the AR and LR primordia (Figure 1B). Although we did not observe any obvious phenotype in the knock out mutants for the AFB1, AFB3, AFB4 and AFB5 proteins we checked their expression during AR initiation using translational fusion lines (Supplemental Figure 3). AFB4:GUS was not at all detected in young seedlings, neither in the dark (Supplemental Figure 3A) nor after transfer to the light for 9 or 72 h (Supplemental Figure 3B and C). AFB5:GUS showed similar profile except an expression in the cotyledons and the root tip in all conditions (Supplemental Figure 3). After transfer to the light the expression of AFB5:GUS extended slightly to the top of the hypocotyl. The absence or very low abundance of AFB4 and AFB5 proteins in the hypocotyl can explain the absence of phenotype in the corresponding mutants and let us conclude that these two proteins do not play a role in the control of AR initiation. In contrast, AFB1:GUS was highly accumulating in the whole seedling at T0 and after transfer to the light (Supplemental Figure 3). Although at a lower level, the AFB3:GUS showed similar expression profile as AFB1 but its level decreased after transfer to the light (Supplemental Figure 3). The absence of phenotype in the *afb1-3* and *afb3-4* loss-of-function mutants cannot be explained by the absence of the proteins but likely by the fact they either target other signaling pathways not related to AR initiation or because they have a very low affinity for the Aux/IAA proteins involved in this process. It was indeed shown that TIR1 and AFB2 exhibit a stronger interaction with selected Aux/IAA than AFB1 and AFB3 (Parry et al., 2009) and that AFB1 and AFB3 had little effect on auxin-dependent Aux/IAA degradation (Havens et al., 2012). Therefore, we conclude that TIR1 and AFB2 are the main Auxin F-box proteins involved in the control of AR initiation.

TIR1 likely controls both JA biosynthesis and conjugation, whereas AFB2 preferentially controls JA conjugation during adventitious root initiation

We previously reported that the AR phenotype was positively correlated with either the amount of GH3 (GH3.3, GH3.5 and GH3.6) proteins (Sorin et al. 2006) or their relative transcript amount (Gutierrez et al., 2012; Pacurar et al., 2014a), therefore based on our model (Supplemental Figure 1A and B), one would expect to see a reduction of the relative transcript

amount of the *GH3* genes in the *tir1-1*, *afb2-3* single mutants and *tir1-1afb2-3* double mutant. Therefore, we analyzed the relative transcript amount of the three *GH3* genes in these mutants (Figure 1C). *GH3-11/JAR1*, which conjugates JA into its bioactive form jasmonoyl-L-isoleucine (JA-Ile), was used as a control. Its expression was only slightly downregulated (40% compared to the wild type) in the *afb2-3* single mutant and *tir1-1afb2-3* double mutant at T72 (Figure 1C), whereas the relative transcript amount of the *GH3* genes was significantly reduced in the *afb2-3* single mutant and *tir1-1afb2-3* double mutant at different time points (Figure 1C).

At T0 only *GH3.3* was significantly downregulated (73% relatively to the wild type) in *tir1-1* while the three *GH3* genes were downregulated in *afb2-3* single mutant (Figure 1C). An additive effect of *tir1-1* mutation was observed for the downregulation of *GH3.3* in the *tir1-1afb2-3* double mutant.

At T9, *GH3.5* and *GH3.6* were significantly downregulated (60% and 40% relatively to the wild type respectively) in *afb2-3* mutant. In contrast, except *GH3.3* which was slightly upregulated (40% relatively to the wild type) in *tir1-1*, the relative transcript amount of the other two genes was unaffected in this mutant. Nevertheless, in the double mutant *tir1-1afb2-3* the relative transcript amount of *GH3.3* and *GH3.5* was significantly decreased compared to the single *afb2-3* mutant suggesting a synergistic effect of the *tir1-1* mutation at this time point.

At T72, only *GH3.3* was slightly (35%) but significantly downregulated in *tir1-1* mutant, while the three *GH3* genes were downregulated in *afb2-3*. As at T9, the relative transcript amount of the *GH3* genes was more affected in the *tir1-1afb2-3* double mutant than in the *afb2-3* single suggesting again a synergistic effect of the two mutations at T72 (Figure 1C).

In conclusion, the relative transcript amount of the *GH3* genes is significantly affected in the *afb2-3* single mutant at all time points, strongly suggesting that AFB2 likely controls AR initiation by regulating JA homeostasis through the *ARF6/ARF8* auxin signaling module (as shown in Supplemental Figure 1). The role of TIR1 in the control of JA conjugation is not as clear, but the synergistic effect on the expression of the *GH3* genes in the double mutant at T9 and T72 suggests that in certain circumstances it also plays a role.

Because AR initiation is affected at the same level in both *tir1-1* and *afb2-3* mutant lines, we hypothesized that TIR1, besides its redundant function in JA conjugation, might have another role in controlling AR initiation by regulating other hormone biosynthesis and/or signaling cascades. To test this hypothesis, we quantified endogenous free salicylic acid (SA), free IAA, free JA and JA-Ile (Figure 2A to D) in the hypocotyls of wild-type seedlings and

seedlings of the *tir1-1*, *afb2-3* single mutants and *tir1-1afb2-3* double mutant. No significant differences in SA content were observed between the wild type and mutants (Figure 2A). A significant increase in free IAA content was observed at T0 in all three mutants compared to the wild type (25% in *tir1-1* and *afb2-3*; 50% in the double mutant; Figure 2B), but only in the *tir1-1afb2-3* double mutant at 9 and 72 hours after transfer to the light (42% increase at T9 and 33% T72; Figure 2B). Takato et al. (2017) have shown that auxin biosynthesis is repressed in a feedback manner by the Aux/IAA and SCF^{TIR1/AFB}-mediated auxin-signaling pathway. Therefore, we conclude that the increase in the free IAA content we observed in the *tir1-1*, *afb2-3* single and *tir1-1afb2-3* double mutants can be explained as a consequence of the downregulation of the auxin signaling pathway which cannot repress the biosynthesis in the mutants

At T0 and T9, a significant increase in free JA was observed in both the *tir1-1* and *afb2-3* single mutants (47% for *tir1-1* and 50% for *afb2-3* at T0; 43% for *tir1-1* and 40% for *afb2-3* at T9) compared to the wild type but not in the double mutant *tir1-1afb2-3* (Figure 2C). The bioactive form JA-Ile was significantly accumulated in the single mutants at all three time points but accumulated only at T9 in the double mutant *tir1-1afb2-3* (Figure 2D). Accumulation of JA and JA-Ile in the *afb2-3* mutant was expected since the three GH3 conjugating enzymes were found to be downregulated (Figure 1C), but we did not *a priori* expect the same level of accumulation for the *tir1-1* mutant which is not strongly affected in the expression of *GH3* genes. Accumulation of JA can be due to a reduction of its conjugation by the GH3 proteins but also to an increase of its biosynthesis. Interestingly it was previously shown that flower buds of auxin receptor mutants produced more JA than the wild-type plants (Cecchetti et al., 2013). Therefore, we checked the expression of JA biosynthesis genes in the mutants to investigate the potential role of TIR1 and/or AFB2 in the control of JA biosynthesis. The relative transcript amounts of seven key genes involved in JA biosynthesis were analyzed by qRT-PCR in the hypocotyls of wild-type, *tir1-1*, *afb2-3* and *tir1-1afb2-3* seedlings grown under adventitious rooting conditions (Figure 3A to C).

At T0, *OPCLI*, *OPR3*, *AOC2* were significantly upregulated (60%, 55% and 73 % respectively relative to the wild type) in the *tir1-1* mutant compared to the wild type, whereas *LOX2* was downregulated (70% relative to the wild type). In the *afb2-3* mutant, no significant differences were observed except for *LOX2* and *AOC1*, which were downregulated compared to the wild type. In the double mutant, *LOX2* and *AOC2* were significantly upregulated (Figure 3A).

Nine hours after transfer to the light (T9), five (*OPCLI*, *OPR3*, *LOX2*, *AOC2*, *AOC3*) out of

the seven biosynthesis genes were significantly upregulated in the single *tir1-1* mutant and four of them (*OPCLI*, *OPR3*, *LOX2*, *AOC2*) were upregulated in the *tir1-lafb2-3* double mutant (Figure 3B), while only *AOC3* and *AOC4* were upregulated in the *afb2-3* mutant (Figure 3B). At T72, only *LOX2* was significantly upregulated in all three mutants (Figure 3C). In conclusion, the *tir1-1* mutation alone has little effect on the expression of the *GH3* genes involved in the conjugation of JA (Figure 1C) but a significant positive effect on the expression of JA biosynthetic genes at T0 and T9. In contrast the *afb2-3* mutation induced a significant downregulation of the *GH3* genes at all time points (Figure 1C) but has little effect on the expression of the JA biosynthesis genes (Figure 3). In addition, we observed a synergistic effect of *tir1-1* mutation when combined with the *afb2-3* mutation since the *GH3* genes were more downregulated in the double mutant than in the single *afb2-3* mutant, suggesting that, in certain circumstances, TIR1 might play a role in the conjugation of JA through the GH3 proteins

The fact that JA and JA-Ile did not accumulate in the double mutant is intriguing as an upregulation of the biosynthesis pathway combined to a downregulation of the conjugation should in contrast lead to an accumulation of JA and JA-Ile. Because too much JA and JA-Ile might become deleterious for the plant, as they inhibit most of the growth processes (reviewed in Huang et al., 2017) a negative feedback loop regulating JA homeostasis by might be set up by the plant to induce the degradation of JA in order to maintain a steady state level. Although significant progress has been made in identifying pathways involved in JA metabolism, their regulation is still poorly understood, and more research is needed to decipher the complexity of these pathways (reviewed in Wasternack and Feussner, 2017)

Therefore, we propose that both TIR1 and AFB2 control JA homeostasis during AR initiation, with a dual role for TIR1 in the control of JA biosynthesis through a pathway yet to be identified and/or conjugation through the *ARF6/ARF8* auxin signaling module depending on the development stage, and a major role for AFB2 in the control of JA conjugation through the *ARF6/ARF8* auxin signaling module.

***IAA6*, *IAA9* and *IAA17* act redundantly to control adventitious root initiation**

ARF6 and *ARF8* are two positive regulators of AR initiation (Gutierrez et al., 2009; Gutierrez et al., 2012) and their transcriptional activity is known to be regulated by Aux/IAA genes. To gain further insight into the auxin sensing machinery and complete our proposed signaling module involved in AR initiation, we attempted to identify potential Aux/IAA proteins that interact with *ARF6* and/or *ARF8*. In 2011, Vernoux *et al.* (2011) conducted a

large-scale analysis of the Aux/IAA-ARF network using a high-throughput yeast two-hybrid approach. They showed that ARF6 and ARF8 belong to a cluster of proteins that can interact with 22 of the 29 Aux/IAA genes (Vernoux et al., 2011). However, this does not help much to restrict the number of genes of interest. Hence, to elucidate which Aux/IAs can interact with ARF6 and ARF8 during AR formation, we looked at those most expressed in the hypocotyl and assessed the expression of the 29 *Aux/IAA* genes in different organs (cotyledons, hypocotyl and roots) of 7-day-old light-grown seedlings using qRT-PCR (Supplemental Figure 4). With the exception of *IAA15*, we detected a transcript for all *IAA* genes in all organs tested (Supplemental Figure 4). Genes with similar expression levels between organs were clustered based on Pearson's correlation, and we observed that, although they were all expressed in the three organs, the profile of expression varied. We observed that 18 *IAA* genes were more expressed in the hypocotyl relatively to cotyledons or roots (*IAA1*, *IAA2*, *IAA3*, *IAA4*, *IAA5*, *IAA6*, *IAA7*, *IAA8*, *IAA9*, *IAA10*, *IAA13*, *IAA14*, *IAA16*, *IAA19*, *IAA26*, *IAA27*, *IAA30*, *IAA31*), 4 *IAA* genes were more expressed in the hypocotyl and the root (*IAA17*, *IAA20*, *IAA28*, *IAA33*) and 6 genes were more expressed in the cotyledons (*IAA11*, *IAA12*, *IAA18*, *IAA29*, *IAA32*, *IAA34*). This differences in the expression pattern certainly contributes to drive a certain specificity of action among the highly redundant *Aux/IAA* genes. To assess the potential contributions of different *IAA* genes in the regulation of AR, we obtained KO mutants available for nine of the *Aux/IAA* genes that displayed a relatively higher expression in the hypocotyl compared to the cotyledons (*iaa3/shy2-24*, *iaa4-1*, *iaa5-1*, *iaa6-1*, *iaa7-1*, *iaa8-1*, *iaa9-1*, *iaa14-1*, *iaa30-1*), two of the genes which had a higher expression in both the hypocotyl and root (*iaa17-6*, *iaa28-1*, *iaa33-1*) and we added two KO mutants with genes whose expression was lower in the hypocotyl and root (*iaa12-1* and *iaa29-1*).

We analyzed AR formation in the *iaa* KO mutants under previously described conditions (Gutierrez et al., 2009; Sorin et al., 2005). Interestingly, six mutants (*iaa5-1*, *iaa6-1*, *iaa7-1*, *iaa8-1*, *iaa9-1* and *iaa17-6*) produced significantly more ARs than the wild type, whereas all the other mutants did not show any significant difference compared to the wild type (Figure 4A). The primary root length and LR number were not affected in mutants *iaa5-1*, *iaa6-1* and *iaa8-1* (Supplemental Figure 2D to F), whereas *iaa9-1* and *iaa17-6* showed a slightly shorter primary root and fewer LRs than the wild type (Supplemental Figure 2D and E) but the LR density was not affected (Supplemental Figure 2F). In contrast, *iaa7-1* had a slightly but significantly longer primary root as well as fewer LRs, which led to a slightly but significantly decreased LR density (Supplemental Figure 2F). These results strongly suggest that *IAA5*, *IAA6*, *IAA7*, *IAA8*, *IAA9* and *IAA17* are involved in the control of AR formation

and substantiate our hypothesis that only a subset of *Aux/IAA* genes regulate the process of AR formation.

Because we found an interaction with ARF6 and/or ARF8 only with the IAA6, IAA9 and IAA17 proteins (see below), we continued to characterize the role of their corresponding genes. All three single *iaa* mutants showed a significant and reproducible AR phenotype. Nevertheless, because extensive functional redundancy has been shown among *Aux/IAA* gene family members (Overvoorde et al., 2005), it was important to confirm the phenotype in at least a second allele (Figure 4B). We also generated the double mutants *iaa6-liaa9-1*, *iaa6-liaa17-6* and *iaa9-liaa17-6* and the triple mutant *iaa6-liaa9-liaa17-6* and analyzed their phenotype during AR formation (Figure 4C). Mutant *iaa4-1* was used as a control showing no AR phenotype. Except for the *iaa6iaa17-6* double mutant, which showed an increased number of AR compared to the single mutants, the other two double mutants were not significantly different from the single mutants (Figure 4C). Nevertheless, we observed a significant increase of the AR number in the triple mutants compared to the double mutants, suggesting that these genes act redundantly in the control of AR initiation (Figure 4C) but do not seem to be involved in the control of the PR or LR root growth as shown on (Supplemental Figure 2G-I). Again, in order to confirm that the growth conditions set for AR initiation do not affect LR development we also analyze the PR and LR development of the triple mutant *iaa6-liaa9-liaa17-6* grown in light conditions only (Supplemental Figure 2J-L) and confirmed the absence of PR and LR phenotype.

We also characterized the expression of IAA6, IAA9 and IAA17 during the early steps of AR formation using transcriptional fusion constructs containing a β -glucuronidase (GUS) coding sequence fused to the respective promoters. At time T0 (i.e., etiolated seedlings prior to transfer to the light) (Figure 4D), *promIAA6:GUS* was strongly expressed in the hypocotyl, slightly less expressed in the cotyledons and only weakly expressed in the root; *promIAA9:GUS* was strongly expressed in the cotyledons, hook and root tips and slightly less in the hypocotyl and root; *promIAA17:GUS* was strongly expressed in the hypocotyl and root, slightly less in the cotyledons and, interestingly, was excluded from the apical hook (Figure 4D). Forty-eight and seventy-two hours after transfer to the light, a decrease in GUS staining was observed for all the lines (Figure 4F and H), but only for IAA9 when the seedlings were kept longer in the dark (Figure 4E and G). These results suggest that light negatively regulates the expression of IAA6 and IAA17 while the expression of IAA9 seem to depend on the developmental stage.

IAA6, IAA9 and IAA17 proteins interact with ARF6 and ARF8 proteins

To establish whether these targeted proteins were effective partners of ARF6 and ARF8, we performed co-immunoprecipitation (CoIP) in protoplasts transfection assays. Arabidopsis protoplasts were transfected with plasmids expressing cMyc- or HA-tagged AuxIAA and ARF proteins according to the protocol described in the Materials and Methods (Magyar et al., 2005). The presence of the putative ARF/AuxIAA complex was tested by western blotting with anti-HA or anti-c-Myc antibodies and only interactions with *IAA6*, *IAA9* and *IAA17* were detected (Figure 5A to E): *IAA6* and *IAA17* interacted with ARF6 and ARF8 (Fig. 5A, B, D and E), whereas *IAA9* interacted only with ARF8 (Figure 5C). These results were confirmed by a bimolecular fluorescence complementation (BiFC) assay (Figure 5I to M)

ARF6 but not ARF8 can form a homodimer

Recent interaction and crystallization studies have shown that ARF proteins dimerize *via* their DNA-binding domain (Boer et al., 2014) and interact not only with Aux/IAA proteins but potentially also with themselves or other ARFs *via* their PB1 domain with a certain specificity (Vernoux et al., 2011). Therefore, we also used CoIP and BiFC assays and tagged versions of the ARF6 and ARF8 proteins to check whether they could form homodimers and/or a heterodimer. Our results (Figure 5G, H, O and P) agreed with a previously published yeast two-hybrid interaction study (Vernoux et al., 2011), which showed that ARF6 and ARF8 do not interact to form a heterodimer and that ARF8 does not homodimerize. In contrast, we showed that ARF6 protein can form a homodimer (Figure 5F and N), suggesting that ARF6 and ARF8, although redundant in controlling the expression of *GH3.3*, *GH3.5* and *GH3.6* genes (Gutierrez et al., 2012), might have a specificity of action.

ARF6, ARF8 and ARF17 are unstable proteins and their degradation is proteasome dependent

While transfecting Arabidopsis protoplasts for CoIP assays with open reading frames encoding individual cMyc- or HA-tagged versions of ARFs and Aux/IAAs, problems were encountered due to instability not only of the tagged Aux/IAA proteins but also of the tagged ARFs. It has previously been reported that like Aux/IAA proteins, ARFs may be rapidly degraded (Salmon et al., 2008). Therefore, we analyzed the degradation of HA₃:ARF6, cMyc₃:ARF8 and HA₃:ARF17. We used HA₃:ARF1, which was previously used as a control (Figure 6A,E,F) (Salmon et al., 2008). Western blot analysis with protein extracts from

transfected protoplasts using anti-HA or anti-cMyc antibodies showed that like ARF1, proteins ARF6, ARF8 and ARF17 were degraded. The HA₃:ARF6 levels decreased dramatically within 30 minutes, indicating that ARF6 is a short-lived protein (Figure 6B), while the degradation rate of HA₃:ARF17 was similar to that of HA₃:ARF1 (Figure 6D) and cMyc₃ARF8 appeared more stable (Figure 6C). To verify whether ARF6, ARF8 and ARF17 proteolysis requires activity of the proteasome for proper degradation, transfected protoplasts were incubated for 2 h in the presence or absence of 50 μ M of a cell permeable proteasome-specific inhibitor, Z-Leu-Leu-Leu-CHO aldehyde (MG132), and the extracted proteins were analyzed by immunoblotting (Figure 6E). The sample incubated with MG132 contained higher levels of HA₃:ARF1, confirming the previously described proteasome-dependent degradation of ARF1 (Salmon et al., 2008), and thereby the efficiency of the treatment. Similarly, HA₃:ARF6, cMyc₃ARF8 and HA₃:ARF17 proteins accumulated in protoplasts treated with MG132, indicating that ARF6, ARF8 and ARF17 degradation is also proteasome dependent (Figure 6E). To further determine whether proteasome activity is necessary for ARF6, ARF8 and ARF17 protein degradation *in vivo*, one-week-old transgenic *in vitro* grown Arabidopsis seedlings expressing HA₃:ARF1, cMyc₃:ARF6, cMyc₃:ARF8 and cMyc₃:ARF17 were treated with MG132 or DMSO for 2 h prior to protein extraction. After western blotting, we observed that levels of HA₃:ARF1, cMyc₃:ARF6, cMyc₃:ARF8 and cMyc₃:ARF17 were enhanced by the addition MG132, confirming that their degradation is proteasome dependent in planta (Figure 6F).

IAA6, IAA9 and IAA17 negatively control expression of GH3.3, GH3.5 and GH3.6

In our model, auxin stimulates adventitious rooting by inducing *GH3.3*, *GH3.5* and *GH3.6* gene expression *via* the positive regulators ARF6 and ARF8 (Supplemental Figure 1). Although we confirmed an interaction between IAA6, IAA9 and IAA17 with ARF6 and/or ARF8, it was important to demonstrate whether disrupting the expression of one of those genes would result in upregulation of *GH3* gene expression. Therefore, we performed qRT-PCR analysis of the relative transcript amounts of the three genes *GH3.3*, *GH3.5*, *GH3.6* in the hypocotyls of single mutants *iaa6-1*, *iaa9-1*, *iaa17-6* first etiolated and then transferred to the light for 72 h. The mutant *iaa4-1*, which had no phenotype affecting AR initiation (Figure 4A), was used as a control. Expression of *GH3.3*, *GH3.5* and *GH3.6* was upregulated in the *iaa9-1* mutant (Figure 7A), whereas only *GH3.3*, *GH3.5* were significantly upregulated in the *iaa6-1* and *iaa17-6* mutant (Figure 7A). In contrast, expression of *GH3.3*, *GH3.5* and *GH3.6* remained unchanged in the *iaa4-1* mutant (Figure 7A). These results confirm that IAA6,

IAA9 and IAA17 are involved in the regulation of adventitious rooting through the modulation of *GH3.3*, *GH3.5* and *GH3.6* expression. To establish whether the *iaa6-1*, *iaa9-1* and *iaa17-6* mutations affected other *GH3* genes, the relative transcript amount of *GH3-10* and *GH3-11* was quantified. Notably, accumulation of *GH3.10* and *GH3.11/JAR1* transcripts was not significantly altered in the *iaa6-1*, *iaa9-1* and *iaa17-6* mutants but *GH3.10* was upregulated in the *iaa4-1* mutant (Figure 7A). We concluded that IAA6, IAA9 and IAA17 negatively regulate *GH3.3*, *GH3.5* and *GH3.6* expression in the Arabidopsis hypocotyl during AR initiation.

We also checked a possible compensatory effect induced by the knockout of one the IAA genes. We performed qRT-PCR analysis of the relative transcript amounts of IAA6, IAA9 and IAA17 genes in the hypocotyl of each single mutant (Figure 7B). Interestingly, a mutation in the IAA6 gene did not affect the expression of IAA9 or IAA17, whereas IAA17 was significantly upregulated in the hypocotyls of *iaa9-1* mutant seedlings. IAA6 was upregulated in the hypocotyl of *iaa17-6* mutant seedlings and a mutation in IAA4 did not affect the expression of any of the three IAA genes of interest (Figure 7B).

DISCUSSION

AR formation is a post-embryonic process that is intrinsic to the normal development of monocots. In both monocots and dicots, it can be induced in response to diverse environmental and physiological stimuli or through horticultural practices used for vegetative propagation of many dicotyledonous species (reviewed in (Bellini et al., 2014; Steffens and Rasmussen, 2016)). Vegetative propagation is widely used in horticulture and forestry for amplification of elite genotypes obtained in breeding programs or selected from natural populations. Although this requires effective rooting of stem cuttings, this is often not achieved, and many studies conducted at physiological, biochemical and molecular levels to better understand the entire process have shown that AR formation is a heritable quantitative genetic trait controlled by multiple endogenous and environmental factors. In particular, it has been shown to be controlled by complex hormone cross-talks, in which auxin plays a central role (reviewed in (Lakehal and Bellini, 2019; Pacurar et al., 2014b)). The specificity of auxin response is thought to depend on a specific combinatorial suite of ARF–Aux/IAA protein–protein interactions from among the huge number of potential interactions that modulate the auxin response of gene promoters via different affinities and activities (reviewed in (Vernoux et al., 2011; Weijers et al., 2005)). In previous work, we identified a regulatory module composed of three *ARF* genes, two activators (*ARF6* and *ARF8*) and one repressor (*ARF17*),

which we showed could control AR formation in *Arabidopsis* hypocotyls (Gutierrez et al., 2009) (Supplemental Figure 1). Recent developments have highlighted the complexity of many aspects of ARF function. In particular, crystallization of the DNA binding domains of ARF1 and ARF5 (Boer et al., 2014) and the C-terminal protein binding domain 1 (PB1) from ARF5 (Nanao et al., 2014) and ARF7 (Korasick et al., 2014) has provided insights into the physical aspects of ARF interactions and demonstrated new perspectives for dimerization and oligomerization that impact ARF functional cooperativity (Parcy et al., 2016). Here, we provide evidence that ARF6 can form a homodimer while we could detect neither heterodimerization between ARF6 and ARF8 nor ARF8 homodimerization. How this influences their respective role in the control of AR initiation is not yet known and requires further investigation. Nevertheless, based on a recent structural analysis of other ARFs (Boer et al., 2014; Parcy et al., 2016), we propose that the ARF6 homodimer would probably target different sites from that of a monomeric ARF8 protein in the *GH3s* promoters, and/or that their respective efficiency of transcriptional regulation would be different, suggesting that one of the two transcription factors might have a prevalent role compared to the other. The prevailing model for auxin-mediated regulation of the Aux/IAA–ARF transcriptional complex is *via* increased Aux/IAA degradation in the presence of auxin, permitting ARF action, possibly through ARF-ARF dimerization, and subsequent regulation of auxin-responsive genes (Nanao et al., 2014; Parcy et al., 2016). As a further step of regulation for auxin-responsive gene transcription, it has been suggested that proteasomal degradation of ARF proteins may be as important as that of Aux/IAA proteins to modulate the ratio between ARFs and Aux/IAs proteins (Salmon et al., 2008). In the present work, we demonstrated that like ARF1 (Salmon et al., 2008), proteins ARF6, ARF8 and ARF17 undergo proteasome dependent degradation. We previously showed that the balance between the two positive regulators ARF6 and ARF8 and the negative regulator ARF17 was important for determining the number of ARs and that this balance was modulated at the post-transcriptional level by the action of the microRNAs miR167 and miR160 (Gutierrez et al., 2009). Here, we suggest that the proteasome dependent degradation of ARF6, ARF8 and ARF17 proteins is an additional level of regulation for modulation of the transcription factor balance during AR formation.

ARF6 and ARF8 (but not ARF17) retain PB1 in their structure, which makes them targets of Aux/IAA repressor proteins. Because most previous genetic studies of *Aux/IAA* genes focused on characterization of gain-of-function mutants and there are only a few recent characterizations of KO mutants (Arase et al., 2012; Shani et al., 2017), we attempted to identify potential Aux/IAA partners involved in the control of AR initiation in the

Arabidopsis hypocotyl. Nevertheless, likely because AR formation is a quantitative trait, we identified six *iaa* KO mutants showing an increased number of ARs. We confirmed direct physical interaction with ARF6 and/or ARF8 for three of them (IAA6, IAA9 and IAA17) and showed significant upregulation of *GH3.3*, *GH3.5* and *GH3.6* expression in the corresponding single KO mutants, confirming that each of the three IAA proteins act as repressors in this pathway. Vernoux *et al.* (2011) also showed interaction between IAA17 and the PB1 domain of ARF6 and ARF8, but in contrast to our results, IAA9 was found to interact with ARF6 and not ARF8. The same study showed interaction of ARF6 and ARF8 with IAA7 and IAA8, which we did not observe when using the full-length proteins. Nevertheless, a KO mutation in *IAA5*, *IAA7* and *IAA8* genes led to a similar phenotype as observed in *iaa6*, *iaa9* and *iaa17* KO mutants. It is therefore possible that IAA5, IAA7 and IAA8 proteins contribute in a combinatorial manner to generate a higher order of oligomerization through interaction with one of the other three Aux/IAA proteins, leading to repression of ARF6 and ARF8 activity. Indeed, Vernoux *et al.* (2011) showed that in the yeast two-hybrid interactome, IAA5, IAA7 and IAA8 interact with IAA6, IAA9 and IAA17. Further, recent work has demonstrated that dimerization of the Aux/IAA repressor with the transcription factor is insufficient to repress the activity and that multimerization is likely to be the mechanism for repressing ARF transcriptional activity (Korasick et al., 2014), which supports our hypothesis. Alternatively, IAA5, IAA7 and IAA8 could contribute to repressing the activity of other ARFs, such as ARF7 and/or ARF19, which have also been shown to be involved in the control of AR formation (Sheng et al., 2017).

In addition to Aux/IAA transcriptional repressors and ARF transcription factors, TIR1/AFB F-box proteins are required for a proper auxin-dependent regulation of transcription. Several elegant studies have shown that auxin promotes degradation of Aux/IAA proteins through the SCF^{TIR1/AFB} in an auxin-dependent manner (Dharmasiri et al., 2005a; Gray et al., 2001; Kepinski and Leyser, 2005; Ramos et al., 2001; Tan et al., 2007). Hence, our model would not be complete without the F-box proteins necessary to release ARF6 and ARF8 transcriptional activity. Among the six TIR1/AFB proteins examined, we demonstrated that TIR1 and AFB2 are the main players involved in this process. Both these proteins act by modulating JA homeostasis since an accumulation of JA and JA-Ile was observed in the single mutants. Nevertheless, our results suggest a different and complementary role for TIR1 and AFB2. Indeed, a mutation in the *TIR1* gene did not affect the expression of the three *GH3* genes in the same way as a mutation in the *AFB2* gene but instead mainly affected the expression of genes involved in JA biosynthesis. These results are

in agreement with a previous study, which showed that TIR1 negatively controls JA biosynthesis during flower development (Cecchetti et al., 2013). Similarly, the loss-of-function *Osd1* mutant in *Oryza sativa*, which accumulated significantly more free-IAA than its wild type counterpart, was found to be defective in JA biosynthesis. All these results indicate that TIR1-dependent auxin signaling may negatively control JA biosynthesis, depending on the developmental stage (Zhao et al., 2013). ARF6 and ARF8 have also been shown to be positive regulators of JA biosynthesis during flower development (Nagpal et al., 2005). However, it is unlikely that TIR1 controls JA biosynthesis through ARF6 and/or ARF8 during AR initiation since ARF6 and ARF8 have been shown to be negative regulators of JA accumulation and by this way positive regulators of AR initiation (Gutierrez et al., 2009; Gutierrez et al., 2012). How TIR1-dependent auxin signaling negatively control JA biosynthesis and which ARF(s) is (are) involved in this process is not known yet and requires further investigation. We are conscious that both gene expression analysis and hormone quantification were performed on whole hypocotyls, at particular time points and therefore may not fully reflect the dynamic of events in the single cells from which the AR initiate. Nevertheless, because our previous work had shown a clear correlation between *GH3* gene expression or protein content in the whole hypocotyl and the number of ARs (Pacurar et al., 2014a; Sorin et al., 2006) on a one hand, and that mutants deficient in JA biosynthesis had an increased number of ARs (Gutierrez et al., 2012) on another hand, we would like to propose here a dual role for TIR1 in the control of AR initiation, i.e., control of JA conjugation through a ARF6/ARF8 signaling module and control of JA biosynthesis through a pathway yet to be identified that would lead to similar amount of endogenous JA and JA isoleucine depending on the developmental stage.

In conclusion, we propose that AR initiation in the *Arabidopsis* hypocotyl depends on regulatory module comprising two F-box proteins (TIR1 and AFB2), at least three Aux/IAA proteins (IAA6, IAA9 and IAA17) and three ARF transcriptional regulators (ARF6, ARF8 and ARF17), which control AR initiation by modulating JA homeostasis, controlling either the conjugation through the *GH3* genes or the biosynthesis through a pathway still to be identified (Figure 7 C and D).

MATERIALS AND METHODS

Plant material and growth conditions

The single mutants *tir1-1*, *afb1-3*, *afb2-3*, *afb3-4*, *afb4-8* and *afb5-5*, multiple mutants *tir1-1afb2-3*, *afb2-3afb3-4*, *afb4-8afb5-5*, *tir1-1afb1-3afb3-4* and, translational fusion lines *tir1-1pTIR1:cTIR1:GUS*, *afb2-3pAFB2:cAFB2:GUS*, *afb1-3pAFB1:cAFB2:GUS* and *afb3-4pAFB3:cAFB3:GUS* were described in (Parry et al., 2009). Seeds of the mutants and transgenic lines including those expressing *pAFB4:cAFB4:GUS* and *pAFB5:cAFB5:GUS* were provided by Prof. Mark Estelle (UCSD, San Diego, CA, USA). The *iaa* T-DNA insertion mutants used in this study are listed in Supplemental Table 1. All the mutants were provided by the Nottingham Arabidopsis Stock Centre, except *iaa3/shy2-24*, which was provided by Prof. Jason Reed (UNC, Chapel Hill, NC, USA). The mutant lines *iaa4-1*, *iaa5-1*, *iaa6-1*, *iaa8-1*, *iaa9-1*, *iaa11-1*, *iaa12-1*, *iaa14-1*, *iaa17-6* and *iaa33-1* were previously described in (Overvoorde et al., 2005). The *Arabidopsis thaliana* ecotype Columbia-0 (Col-0) was used as the wild type and background for all the mutants and transgenic lines, except *iaa3/shy2-24*, which had a Landsberg *erecta* (Ler) background. Growth conditions and adventitious rooting experiments were performed as previously described (Gutierrez et al., 2009; Sorin et al., 2005).

Hormone profiling experiment

Hypocotyls from the wild type Col-0, single mutants *tir1-1* and *afb2-3* and double mutant *tir1-1afb2-3* were collected from seedlings grown as described in (Gutierrez et al., 2012). Samples were prepared from six biological replicates; for each, at least 2 technical replicates were used. Endogenous levels of free IAA, SA and JA as well as the conjugated form of JA, JA-Ile, were determined in 20 mg of hypocotyls according to the method described in (Flokova et al., 2014). The phytohormones were extracted using an aqueous solution of methanol (10% MeOH/H₂O, v/v). To validate the LC-MS method, a cocktail of stable isotope-labeled standards was added with the following composition: 5 pmol of [¹³C₆]IAA, 10 pmol of [²H₆]JA, [²H₂]JA-Ile and 20 pmol of [²H₄]SA (all from Olchemim Ltd, Czech Republic) per sample. The extracts were purified using Oasis HLB columns (30 mg/1 ml, Waters, Milford, MA, USA) and targeted analytes were eluted using 80% MeOH. Eluent containing neutral and acidic compounds was gently evaporated to dryness under a stream of nitrogen. Separation was performed on an Acquity UPLC® System (Waters, Milford, MA, USA) equipped with an Acquity UPLC BEH C18 column (100 x 2.1 mm, 1.7 µm; Waters,

Milford, MA, USA), and the effluent was introduced into the electrospray ion source of a triple quadrupole mass spectrometer Xevo™ TQ-S MS (Waters, Milford, MA, USA).

RNA isolation and cDNA Synthesis

RNAs from the hypocotyls of Col-0 and the mutants were prepared as described by (Gutierrez et al., 2009; Gutierrez et al., 2012). The resulting RNA preparations were treated with DNaseI using a DNAfree Kit (ThermoFisher Scientific AM1906; <https://www.thermofisher.com>) and cDNA was synthesized by reverse transcribing 2 µg of total RNA using SuperScript III reverse transcriptase (ThermoFisher Scientific 18064-014; <https://www.thermofisher.com>) with 500 ng of oligo(dT)18 primer according to the manufacturer's instructions. The reaction was stopped by incubation at 70°C for 10 min, and then the reaction mixture was treated with RNaseH (ThermoFisher Scientific EN0201; <https://www.thermofisher.com>) according to the manufacturer's instructions. All cDNA samples were tested by PCR using specific primers flanking an intron sequence to confirm the absence of genomic DNA contamination.

Quantitative RT-PCR experiments

Transcript levels were assessed in three independent biological replicates by real-time qRT-PCR), in assays with triplicate reaction mixtures (final volume 20 µl) containing 5 µl of cDNA, 0.5 µM of both forward and reverse primers and 1 X FastStart SYBR Green Master mix (Roche Ref: 04887352001; <https://lifescience.roche.com>). Steady state levels of transcripts were quantified using primers listed in Supplemental Table 2. *APT1* and *TIP41* had previously been validated as the most stably expressed genes among 11 tested in our experimental procedures and were used to normalize the qRT-PCR data (Gutierrez et al., 2009). The normalized expression patterns obtained using the reference genes were similar. Therefore, only data normalized with *TIP41* are shown. The CT (crossing threshold value) and PCR efficiency (*E*) values were used to calculate expression using the formula $E_T^{(CT_{WT} - CT_M)}/E_R^{(CT_{WT} - CT_M)}$, where T is the target gene, R is the reference gene, M refers to cDNA from the mutant line and WT refers to cDNA from the wild type. Data for the mutants were presented relative to those of the wild type, the calibrator.

Heatmap of AUXIAA gene expression

AUXIAA gene expression values were obtained as described previously in different organs (cotyledons, hypocotyls and roots). The *AUXIAA* expression values for hypocotyls and roots

were calculated relative to those of the cotyledon samples as calibrator and set as 1. These values were subsequently used to build a cluster heatmap using Genesis software (<http://www.mybiosoftware.com/genesis-1-7-6-cluster-analysis-microarray-data.html>) (Sturn et al., 2002). Genes with similar expression levels between organs were clustered based on Pearson's correlation. Correlation values near 1 indicated a strong positive correlation between two genes.

Tagged protein constructs

Epitope-tagged versions of ARF6, ARF8, ARF17, IAA5, IAA6, IAA7, IAA8, IAA9 and IAA17 proteins were produced in pRT104-3xHA and pRT104-3xMyc plasmids (Fulop et al., 2005). All plasmids displayed a 35S promoter sequence upstream of the multi-cloning site. The open reading frames of *ARF6*, *ARF8*, *ARF17*, *IAA5*, *IAA6*, *IAA7*, *IAA8*, *IAA9* and *IAA17* were amplified from cDNA from 7-day-old *Arabidopsis* seedlings using Finnzyme's Phusion high-fidelity DNA polymerase (ThermoFisher SCIENTIFIC, F530S) protocol with gene-specific primers listed in *SI Appendix* Table S3.

For the bimolecular functional complementation assay (BiFC), the open reading frames of *ARF6*, *ARF8*, *IAA6*, *IAA9* and *IAA17* were amplified with gene-specific primers carrying BgIII or KpnI restriction sites to facilitate subsequent cloning (*SI Appendix* Table S4). The products obtained after PCR were digested with BgIII and KpnI prior to ligation into pSAT-nEYFP and pSAT-cEYFP plasmids (Citovsky et al., 2006) that had previously been cut open with the same enzymes. All constructs were verified by sequencing.

Protoplast production and transformation

Protoplasts from *Arabidopsis* cell culture or 14-day-old *Arabidopsis* seedlings were prepared and transfected as previously described (Meskiene et al., 2003; Zhai et al., 2009). For CoIP, 10⁵ protoplasts from the *Arabidopsis* cell culture were transfected with 5 to 7.5 µg of each construct.

For BiFC assays, *Arabidopsis* mesophyll protoplasts were co-transfected with 10 µg of each construct. The protoplasts were imaged by confocal laser scanning microscopy after 24 hours of incubation in the dark at room temperature.

Co-immunoprecipitation

For testing protein interactions, co-transfected protoplasts were extracted in lysis buffer containing 25 mM Tris-HCl, pH 7.8, 10 mM MgCl₂, 75 mM NaCl, 5 mM EGTA, 60 mM β-

glycerophosphate, 1 mM dithiothreitol, 10% glycerol, 0.2% Igepal CA-630 and Protein Inhibitor Cocktail (Sigma-Aldrich P9599-5ML; <http://www.sigmaaldrich.com/>). The cell suspension was frozen in liquid nitrogen and then thawed on ice and centrifuged for 5 min at 150 g. The resulting supernatant was mixed with 1.5 µl of anti-Myc antibody (9E10, Covance; <http://www.covance.com/>) or 2 µl of anti-HA antibody (16B12, Covance; <http://www.covance.com/>) for 2 h at 4°C on a rotating wheel. Immunocomplexes were captured on 10 µl of Protein G-Sepharose beads (GE Healthcare, 17-0618-01), washed three times in 25 mM sodium phosphate, 5% glycerol and 0.2% Igepal CA-630 buffer and then eluted by boiling with 40 µl of SDS sample buffer. The presence of immunocomplexes was assessed by probing protein gel blots with either anti-HA (3F10, Sigma/Roche; <http://www.sigmaaldrich.com/>) or anti-Myc antibody (9E10, Covance; <http://www.covance.com/>) at 1:2000 dilution.

Cycloheximide or proteasome inhibitor treatment of transfected protoplasts

Sixteen hours after protoplast transfection, cycloheximide (CHX) (SigmaAldrich C7698-1G; <http://www.sigmaaldrich.com/>) was added to a final concentration of 200 µg/ml in the protoplast growth medium and the protoplasts were incubated for 0, 0.5, 1, 1.5 and 2 h. Afterwards, the protoplasts were harvested and the proteins extracted and analyzed by SDS-PAGE and western blotting.

The proteasome inhibitor MG132 (SigmaAldrich M7449, http://www.sigmaaldrich.com) was applied at a concentration of 50 µM 16 h after protoplasts transfection. After 2 h incubation, the protoplasts were harvested, and the proteins were extracted and analyzed by SDS-PAGE and western blotting. The plasmid expressing *HA₃-ARF1* was described in (Salmon et al., 2008) and kindly provided by Prof. Judy Callis (UC, Davis, CA, USA).

Proteasome inhibition in planta

Seeds from Arabidopsis lines expressing HA₃:ARF1, cMyc₃:ARF6, cMyc₃:ARF8 and cMyc₃:ARF17 were sterilized and sown *in vitro* as previously described (Sorin et al., 2005). Plates were incubated at 4°C for 48 h for stratification and transferred to the light for 16 h at a temperature of 20°C to induce germination. The plates were then wrapped in aluminum foil and kept until the hypocotyl of the seedlings reached on average 6 mm. The plates were then transferred back to the light for 6 days. On day 6, the seedlings were transferred to liquid growth medium (GM). On day 7, the GM was removed and fresh GM without (DMSO

control) or with MG132 (SigmaAldrich M7449, <http://www.sigmaaldrich.com/>) at a final concentration of 100 μ M was added, and the seedlings incubated for a further 2 h. After incubation, the GM liquid culture was removed, and proteins were extracted and analyzed by SDS-PAGE and western blotting. The Arabidopsis line expressing *HA₃-ARF1* was described in (Salmon et al., 2008) and kindly provided by Prof. Judy Callis (UC, Davis, CA, USA).

Analysis of promoter activity

A 1-kb-long fragment upstream from the start codon of *IAA6*, *IAA9* and *IAA17* was amplified by applying PCR to Col-0 genomic DNA. The primer sequences used are listed in *SI Appendix* Table S5. The amplified fragments were cloned using a pENTR/D-TOPO cloning kit (ThermoFisher Scientific K240020; <https://www.thermofisher.com>) and transferred into the pKGWFS7 binary vector (Karimi et al., 2002) using a Gateway LR Clonase enzyme mix (ThermoFisher Scientific 11791020; <https://www.thermofisher.com>) according to the manufacturer's instructions. Transgenic Arabidopsis plants expressing the *promIAA6:GUS*, *promIAA9:GUS* and *promIAA17:GUS* fusion were generated by *Agrobacterium tumefaciens* mediated floral dipping and the expression pattern was checked in the T2 progeny of several independent transgenic lines. Histochemical assays of GUS expression were performed as previously described (Sorin et al., 2005).

Confocal laser scanning microscopy

For the BIFC assay, images of fluorescent protoplasts were obtained with a Leica TCS-SP2-AOBS spectral confocal laser scanning microscope equipped with a Leica HC PL APO x 20 water immersion objective. YFP and chloroplasts were excited with the 488 nm line of an argon laser (laser power 35%). Fluorescence emission was detected over the range 495 to 595 nm for the YFP construct and 670 to 730 nm for chloroplast autofluorescence. Images were recorded and processed using LCS software version 2.5 (Leica Microsystems). Images were cropped using Adobe Photoshop CS2 and assembled using Adobe Illustrator CS2 software (Adobe, <http://www.adobe.com>).

ACKNOWLEDGMENTS

The authors would like to thank Prof. Mark Estelle (UCSD, San Diego, CA, USA) and Prof Jason Reed (UNC, Chapel Hill, NC, USA) for providing seeds of single and multiple mutants. The authors also thank Prof. Judy Callis (UC, Davis, CA, USA) for providing Arabidopsis

line and the plasmid expressing *HA₃-ARF1*. We also thank Hana Martinková for help with phytohormone analyses. This work was supported by the Swedish Research Council (VR), the Swedish Research Council for Research and Innovation for Sustainable Growth (VINNOVA), the K. & A. Wallenberg Foundation, the Carl Trygger Foundation, the Carl Kempe Foundation to C. B., the University of Picardie Jules Verne, the Regional Council of Picardie to L.G., the European Regional Development Fund, and the Ministry of Education, Youth and Sports of the Czech Republic (European Regional Development Fund-Project “Plants as a tool for sustainable global development” no. CZ.02.1.01/0.0/0.0/16_019/0000827) to O.N..

ATHORS CONTRIBUTION

Methodology, A.L., C.B., E.C. and S.C.; Investigation, A.L., S.C., E.C., R.L.H., Z.R., O.N., F.J., D.I.P., I.P., A.R., L.G., L.B.; Writing-original draft, A.L., S.C. and C.B; Writing-Review & Editing, A.L., C.B., E.C., L.G., R.L.H., L.B., O.N.; Conceptualization C.B.; Supervision C.B.; Funding Acquisition, C.B., L.G. and O.N.

REFERENCES

- Arase, F., Nishitani, H., Egusa, M., Nishimoto, N., Sakurai, S., Sakamoto, N., and Kaminaka, H.** (2012). IAA8 involved in lateral root formation interacts with the TIR1 auxin receptor and ARF transcription factors in Arabidopsis. *PLoS One* **7**:e43414.
- Bellini, C., Pacurar, D.I., and Perrone, I.** (2014). Adventitious roots and lateral roots: similarities and differences. *Annu. Rev. Plant Biol.* **65**:639-666.
- Boer, D.R., Freire-Rios, A., van den Berg, W.A., Saaki, T., Manfield, I.W., Kepinski, S., Lopez-Vidrieo, I., Franco-Zorrilla, J.M., de Vries, S.C., Solano, R., et al.** (2014). Structural basis for DNA binding specificity by the auxin-dependent ARF transcription factors. *Cell* **156**:577-589.
- Calderon Villalobos, L.I., Lee, S., De Oliveira, C., Ivetac, A., Brandt, W., Armitage, L., Sheard, L.B., Tan, X., Parry, G., Mao, H., et al.** (2012). A combinatorial TIR1/AFB-Aux/IAA co-receptor system for differential sensing of auxin. *Nat. Chem. Biol.* **8**:477-485.
- Cecchetti, V., Altamura, M.M., Brunetti, P., Petrocelli, V., Falasca, G., Ljung, K., Costantino, P., and Cardarelli, M.** (2013). Auxin controls Arabidopsis anther dehiscence by regulating endothecium lignification and jasmonic acid biosynthesis. *Plant J.* **74**:411-422.
- Chapman, E.J., and Estelle, M.** (2009). Mechanism of auxin-regulated gene expression in plants. *Annu. Rev. Genet.* **43**:265-285.
- Citovsky, V., Lee, L.Y., Vyas, S., Glick, E., Chen, M.H., Vainstein, A., Gafni, Y., Gelvin, S.B., and Tzfira, T.** (2006). Subcellular localization of interacting proteins by bimolecular fluorescence complementation in planta. *J. Mol. Biol.* **362**:1120-1131.
- De Rybel, B., Vassileva, V., Parizot, B., Demeulenaere, M., Grunewald, W., Audenaert, D., Van Campenhout, J., Overvoorde, P., Jansen, L., Vanneste, S., et al.** (2010). A novel aux/IAA28 signaling cascade activates GATA23-dependent specification of lateral root founder cell identity. *Curr. Biol.* **20**:1697-1706.
- De Smet, I., Lau, S., Voss, U., Vanneste, S., Benjamins, R., Rademacher, E.H., Schlereth, A., De Rybel, B., Vassileva, V., Grunewald, W., et al.** (2010). Bimodular auxin response controls organogenesis in Arabidopsis. *Proc. Natl. Acad. Sci. U S A* **107**:2705-2710.

787 **Dello Ioio, R., Nakamura, K., Moubayidin, L., Perilli, S., Taniguchi, M., Morita, M.T.,**
788 **Aoyama, T., Costantino, P., and Sabatini, S. (2008).** A genetic framework for the
789 control of cell division and differentiation in the root meristem. *Science* **322**:1380-1384.

790 **Dharmasiri, N., Dharmasiri, S., and Estelle, M. (2005a).** The F-box protein TIR1 is an
791 auxin receptor. *Nature* **435**:441-445.

792 **Dharmasiri, N., Dharmasiri, S., Weijers, D., Lechner, E., Yamada, M., Hobbie, L.,**
793 **Ehrismann, J.S., Jurgens, G., and Estelle, M. (2005b).** Plant development is
794 regulated by a family of auxin receptor F box proteins. *Dev. Cell.* **9**:109-119.

795 **Flokova, K., Tarkowska, D., Miersch, O., Strnad, M., Wasternack, C., and Novak, O.**
796 **(2014).** UHPLC-MS/MS based target profiling of stress-induced phytohormones.
797 *Phytochemistry* **105**:147-157.

798 **Fukaki, H., Tameda, S., Masuda, H., and Tasaka, M. (2002).** Lateral root formation is
799 blocked by a gain-of-function mutation in the SOLITARY-ROOT/IAA14 gene of
800 *Arabidopsis*. *Plant J.* **29**:153-168.

801 **Fulop, K., Pettko-Szandtner, A., Magyar, Z., Miskolczi, P., Kondorosi, E., Dudits, D.,**
802 **and Bako, L. (2005).** The Medicago CDKC;1-CYCLINT;1 kinase complex
803 phosphorylates the carboxy-terminal domain of RNA polymerase II and promotes
804 transcription. *Plant J.* **42**:810-820.

805 **Geiss, G., Gutierrez, L., and Bellini, C. (2009).** Adventitious root formation: new insights
806 and perspective. In: *Root Development - Annual Plant Reviews --Beeckman, T., ed.*
807 London: A John Wiley & Sons, Ltd. 127-156.

808 **Gray, W.M., Kepinski, S., Rouse, D., Leyser, O., and Estelle, M. (2001).** Auxin regulates
809 SCF(TIR1)-dependent degradation of AUX/IAA proteins. *Nature* **414**:271-276.

810 **Guilfoyle, T.J., and Hagen, G. (2007).** Auxin response factors. *Curr. Opin. Plant Biol.*
811 **10**:453-460.

812 **Guilfoyle, T.J., and Hagen, G. (2012).** Getting a grasp on domain III/IV responsible for
813 Auxin Response Factor-IAA protein interactions. *Plant Sci.* **190**:82-88.

814 **Gutierrez, L., Bussell, J.D., Pacurar, D.I., Schwambach, J., Pacurar, M., and Bellini, C.**
815 **(2009).** Phenotypic plasticity of adventitious rooting in *Arabidopsis* is controlled by
816 complex regulation of AUXIN RESPONSE FACTOR transcripts and microRNA
817 abundance. *Plant Cell* **21**:3119-3132.

818 **Gutierrez, L., Mongelard, G., Flokova, K., Pacurar, D.I., Novak, O., Staswick, P.,**
819 **Kowalczyk, M., Pacurar, M., Demailly, H., Geiss, G., et al. (2012).** Auxin controls

Arabidopsis adventitious root initiation by regulating jasmonic acid homeostasis. *Plant Cell* **24**:2515-2527.

Hamann, T., Benkova, E., Baurle, I., Kientz, M., and Jurgens, G. (2002). The Arabidopsis BODENLOS gene encodes an auxin response protein inhibiting MONOPTEROS-mediated embryo patterning. *Genes Dev.* **16**:1610-1615.

Havens, K.A., Guseman, J.M., Jang, S.S., Pierre-Jerome, E., Bolten, N., Klavins, E. and Nemhauser, J. (2012) A Synthetic Approach Reveals Extensive Tunability of Auxin Signaling. *Plant Phys.* **160**: 135-142

Karimi, M., Inze, D., and Depicker, A. (2002). GATEWAY vectors for Agrobacterium-mediated plant transformation. *Trends Plant Sci.* **7**:193-195.

Kepinski, S., and Leyser, O. (2005). The Arabidopsis F-box protein TIR1 is an auxin receptor. *Nature* **435**:446-451.

Korasick, D.A., Westfall, C.S., Lee, S.G., Nanao, M.H., Dumas, R., Hagen, G., Guilfoyle, T.J., Jez, J.M., and Strader, L.C. (2014). Molecular basis for AUXIN RESPONSE FACTOR protein interaction and the control of auxin response repression. *Proc. Natl. Acad. Sci. U S A* **111**:5427-5432.

Lakehal, A., and Bellini, C. (2019). Control of adventitious root formation: insights into synergistic and antagonistic hormonal interactions. *Physiol Plant.* **165**:90-100.

Lavenus, J., Goh, T., Roberts, I., Guyomarc'h, S., Lucas, M., De Smet, I., Fukaki, H., Beeckman, T., Bennett, M., and Laplaze, L. (2013). Lateral root development in Arabidopsis: fifty shades of auxin. *Trends Plant Sci.* **18**:450-458.

Magyar, Z., De Veylder, L., Atanassova, A., Bako, L., Inze, D., and Bogre, L. (2005). The role of the Arabidopsis E2FB transcription factor in regulating auxin-dependent cell division. *Plant Cell* **17**:2527-2541.

Meskiene, I., Baudouin, E., Schweighofer, A., Liwosz, A., Jonak, C., Rodriguez, P.L., Jelinek, H., and Hirt, H. (2003). Stress-induced protein phosphatase 2C is a negative regulator of a mitogen-activated protein kinase. *J. Biol. Chem.* **278**:18945-18952.

Nagpal, P., Ellis, C.M., Weber, H., Ploense, S.E., Barkawi, L.S., Guilfoyle, T.J., Hagen, G., Alonso, J.M., Cohen, J.D., Farmer, E.E., et al. (2005). Auxin response factors ARF6 and ARF8 promote jasmonic acid production and flower maturation. *Development* **132**:4107-4118.

Nanao, M.H., Vinos-Poyo, T., Brunoud, G., Thevenon, E., Mazzoleni, M., Mast, D., Laine, S., Wang, S., Hagen, G., Li, H., et al. (2014). Structural basis for oligomerization of auxin transcriptional regulators. *Nat. Commun.* **5**:3617.

854 **Okushima, Y., Overvoorde, P. J., Arima, K., Alonso, J. M., Chan, A., Chang, C., Ecker,**
855 **J. R., Hughes, B., Lui, A., et al. (2005).** Functional genomic analysis of the AUXIN
856 RESPONSE FACTOR gene family members in *Arabidopsis thaliana*: unique and
857 overlapping functions of ARF7 and ARF19. *Plant Cell* **17**: 444-463

858 **Orosa-Puente, B., Leftley, N., von Wangenheim, D., Banda, J., Srivastava, A.K., Hill, K.,**
859 **Truskina, J., Bhosale, R., Morris, E., Srivastava, M., et al. (2018).** Root branching
860 toward water involves posttranslational modification of transcription factor ARF7.
861 *Science* **362**:1407-1410.

862 **Overvoorde, P.J., Okushima, Y., Alonso, J.M., Chan, A., Chang, C., Ecker, J.R.,**
863 **Hughes, B., Liu, A., Onodera, C., Quach, H., et al. (2005).** Functional genomic
864 analysis of the AUXIN/INDOLE-3-ACETIC ACID gene family members in
865 *Arabidopsis thaliana*. *Plant Cell* **17**:3282-3300.

866 **Pacurar, D.I., Pacurar, M.L., Bussell, J.D., Schwambach, J., Pop, T.I., Kowalczyk, M.,**
867 **Gutierrez, L., Cavel, E., Chaabouni, S., Ljung, K., et al. (2014a).** Identification of
868 new adventitious rooting mutants amongst suppressors of the *Arabidopsis thaliana*
869 superroot2 mutation. *J Exp Bot* **65**:1605-1618.

870 **Pacurar, D.I., Perrone, I., and Bellini, C. (2014b).** Auxin is a central player in the hormone
871 cross-talks that control adventitious rooting. *Physiol. Plant.* **151**:83-96.

872 **Parcy, F., Vernoux, T., and Dumas, R. (2016).** A Glimpse beyond Structures in Auxin-
873 Dependent Transcription. *Trends Plant Sci.* **21**:574-583.

874 **Parry, G., Calderon-Villalobos, L.I., Prigge, M., Peret, B., Dharmasiri, S., Itoh, H.,**
875 **Lechner, E., Gray, W.M., Bennett, M., and Estelle, M. (2009).** Complex regulation
876 of the TIR1/AFB family of auxin receptors. *Proc. Natl. Acad. Sci. U S A* **106**:22540-
877 22545.

878 **Ramos, J.A., Zenser, N., Leyser, O., and Callis, J. (2001).** Rapid degradation of
879 auxin/indoleacetic acid proteins requires conserved amino acids of domain II and is
880 proteasome dependent. *Plant Cell* **13**:2349-2360.

881 **Salmon, J., Ramos, J., and Callis, J. (2008).** Degradation of the auxin response factor
882 ARF1. *Plant J.* **54**:118-128.

883 **Shani, E., Salehin, M., Zhang, Y., Sanchez, S.E., Doherty, C., Wang, R., Mangado, C.C.,**
884 **Song, L., Tal, I., Pisanty, O., et al. (2017).** Plant Stress Tolerance Requires Auxin-
885 Sensitive Aux/IAA Transcriptional Repressors. *Curr. Biol.* **27**:437-444.

- 886 **Sheng, L., Hu, X., Du, Y., Zhang, G., Huang, H., Scheres, B., and Xu, L.** (2017). Non-
887 canonical WOX11-mediated root branching contributes to plasticity in Arabidopsis root
888 system architecture. *Development* **144**:3126-3133.
- 889 **Sorin, C., Bussell, J.D., Camus, I., Ljung, K., Kowalczyk, M., Geiss, G., McKhann, H.,**
890 **Garcion, C., Vaucheret, H., Sandberg, G., et al.** (2005). Auxin and light control of
891 adventitious rooting in Arabidopsis require ARGONAUTE1. *Plant Cell* **17**:1343-1359.
- 892 **Sorin, C., Negroni, L., Balliau, T., Corti, H., Jacquemot, M.P., Davanture, M.,**
893 **Sandberg, G., Zivy, M., and Bellini, C.** (2006). Proteomic analysis of different mutant
894 genotypes of Arabidopsis led to the identification of 11 proteins correlating with
895 adventitious root development. *Plant Physiol* **140**:349-364.
- 896 **Staswick, P.E., Serban, B., Rowe, M., Tiriyaki, I., Maldonado, M.T., Maldonado, M.C.,**
897 **and Suza, W.** (2005) Characterization of an Arabidopsis enzyme family that conjugates
898 amino acids to indole-3-acetic acid. *Plant Cell* **17**: 616–627
- 899 **Steffens, B., and Rasmussen, A.** (2016). The Physiology of Adventitious Roots. *Plant*
900 *Physiol* **170**:603-617.
- 901 **Sturn, A., Quackenbush, J., and Trajanoski, Z.** (2002). Genesis: cluster analysis of
902 microarray data. *Bioinformatics* **18**:207-208.
- 903 **Sun, J., Qi, L., Li, Y., Zhai, Q., and Li, C.** (2013). PIF4 and PIF5 transcription factors link
904 blue light and auxin to regulate the phototropic response in Arabidopsis. *Plant Cell*
905 **25**:2102-2114.
- 906 **Szemenyei, H., Hannon, M., and Long, J.A.** (2008). TOPLESS mediates auxin-dependent
907 transcriptional repression during Arabidopsis embryogenesis. *Science* **319**:1384-1386.
- 908 **Takato, S., Kakei, Y., Mitsui, M., Ishida, Y., Suzuki, M., Yamazaki, C., Hayashi, K. I.,**
909 **Ishii, T., Nakamura, A., Soeno, K., and Shimada, Y.** (2017) Auxin signaling through
910 SCF(TIR1/AFBs) mediates feedback regulation of IAA biosynthesis. *Biosci.*
911 *Biotechnol. Biochem.* **81**: 320-1326
- 912 **Tan, X., Calderon-Villalobos, L.I., Sharon, M., Zheng, C., Robinson, C.V., Estelle, M.,**
913 **and Zheng, N.** (2007). Mechanism of auxin perception by the TIR1 ubiquitin ligase.
914 *Nature* **446**:640-645.
- 915 **Tatematsu, K., Kumagai, S., Muto, H., Sato, A., Watahiki, M.K., Harper, R.M., Liscum,**
916 **E., and Yamamoto, K.T.** (2004). MASSUGU2 encodes Aux/IAA19, an auxin-
917 regulated protein that functions together with the transcriptional activator NPH4/ARF7
918 to regulate differential growth responses of hypocotyl and formation of lateral roots in
919 *Arabidopsis thaliana*. *Plant Cell* **16**:379-393.

- Vernoux, T., Brunoud, G., Farcot, E., Morin, V., Van den Daele, H., Legrand, J., Oliva, M., Das, P., Larrieu, A., Wells, D., et al.** (2011). The auxin signalling network translates dynamic input into robust patterning at the shoot apex. *Mol. Syst. Biol.* **7**:508.
- Wang, H., Jones, B., Li, Z., Frasse, P., Delalande, C., Regad, F., Chaabouni, S., Latche, A., Pech, J.C., and Bouzayan, M.** (2005). The tomato Aux/IAA transcription factor IAA9 is involved in fruit development and leaf morphogenesis. *Plant Cell* **17**:2676-2692.
- Wang, R., and Estelle, M.** (2014). Diversity and specificity: auxin perception and signaling through the TIR1/AFB pathway. *Curr. Opin. Plant Biol.* **21**:51-58.
- Wasternack, C. and Feussner, I.** (2017) The Oxylin Pathways: Biochemistry and Function. *Annu. Rev. Plant Biol.* **69**:363-386
- Weijers, D., Sauer, M., Meurette, O., Friml, J., Ljung, K., Sandberg, G., Hooykaas, P., and Offringa, R.** (2005). Maintenance of embryonic auxin distribution for apical-basal patterning by PIN-FORMED-dependent auxin transport in Arabidopsis. *Plant Cell* **17**:2517-2526.
- Weijers, D., and Wagner, D.** (2016). Transcriptional Responses to the Auxin Hormone. *Annu. Rev. Plant Biol.* **67**:539-574.
- Xuan, W., Audenaert, D., Parizot, B., Moller, B. K., Njo, M. F., De Rybel, B., De Rop, G., Van Isterdael, G., Mahonen, A. P et al.** (2015) Root Cap-Derived Auxin Pre-patterns the Longitudinal Axis of the Arabidopsis Root. *Curr. Biol.* **25**:1381-1388
- Zhai, Z., Jung, H.I., and Vatamaniuk, O.K.** (2009). Isolation of protoplasts from tissues of 14-day-old seedlings of Arabidopsis thaliana. *J. Vis. Exp.* **30**:1149
- Zhao, Z., Zhang, Y., Liu, X., Zhang, X., Liu, S., Yu, X., Ren, Y., Zheng, X., Zhou, K., Jiang, L. et al.** (2013) A role for a dioxygenase in auxin metabolism and reproductive development in rice. *Dev. Cell* **27**:113-122

FIGURE LEGENDS

Figure 1: TIR1 and AFB2 control adventitious root initiation by modulating *GH3.3*, *GH3.5* and *GH3.6* expression

(A) Average numbers of adventitious roots in *tir1/afb* mutants. Seedlings were first etiolated in the dark until their hypocotyls were 6 mm long and then transferred to the light for 7 days. Data were obtained from 3 biological replicates; for each, data for at least 30 seedlings were pooled and averaged. Errors bars indicate \pm SE. A non-parametric Kruskal-Wallis test followed by the Dunn's multiple comparison post-test indicated that only mutations in the *TIR1* and *AFB2* genes significantly affected the initiation of adventitious roots ($n > 30$; $P < 0.001$).

(B) Expression pattern of TIR1 and AFB2 proteins. GUS staining of *tir1-1pTIR1::cTIR1-GUS* and *afb2-3pAFB2::cAFB2-GUS* translational fusions (arranged from left to right in each panel) in seedlings grown in the dark until their hypocotyls were 6 mm long (T0) and 9 h (T9) and 72 h (T72) after their transfer to the light. (a) and (b) Close-ups from hypocotyl regions shown for T72. Scale bar = 2 mm

(C) Quantification by qRT-PCR of *GH3.3*, *GH3.5* and *GH3.6* transcripts in hypocotyls of *tir1-1* and *afb2-3* single mutants and the *tir1-1afb2-3* double mutant. mRNAs were extracted from hypocotyls of seedlings grown in the dark until the hypocotyl reached 6 mm (T0) and after their transfer to the light for 9 h or 72 h. The gene expression values are relative to the expression in the wild type, for which the value was set to 1. The scale is a log₁₀ scale, the extremum and minimum of each graph have been optimized according to the expression values. Error bars indicate \pm SE obtained from three independent biological replicates. One-way ANOVA combined with Dunnett's multiple comparison test indicated that in some cases, the relative amount of mRNA was significantly different from the wild type (denoted by *, $P < 0.001$; $n = 3$).

Figure 2: TIR1 and AFB2 control adventitious root initiation by modulating jasmonate homeostasis

(A) to (D) The endogenous contents of free IAA (D), free SA (B), free JA (C) and JA-Ile (D) were quantified in the hypocotyls of wild type Col-0, single mutants *tir1-1* and *afb2-3* and double mutant *tir1-1afb2-3* seedlings grown in the dark until the hypocotyl reached 6 mm (T0) and after their transfer to the light for 9 h (T9) or 72 h (T72). Error bars indicate \pm SD of six biological replicates. One-way ANOVA combined with Dunnett's multiple comparison test indicated that in some cases, values were significantly different from those of the wild-

type Col-0 (denoted by *, $P < 0.05$; $n = 6$).

Figure 3: A mutation in TIR1 induces an upregulation of the JA biosynthesis genes

(A) to (C) Relative transcript amount of genes involved in JA biosynthesis (*OPCLI*, *OPR3*, *LOX2*, *AOC1*, *AOC2*, *AOC3*, *AOC4*). The transcript amount was assessed by qRT-PCR using mRNAs extracted from hypocotyls of seedlings grown in the dark until the hypocotyl reached 6 mm (T0) and after their transfer to the light for 9 h (T9) or 72 h (T72). The gene expression values are relative to the expression in the wild type, for which the value was set to 1. Error bars indicate \pm SE obtained from three independent biological replicates. The scale is a log10 scale, the extremum and minimum of each graph have been optimized according to the expression values. One-way ANOVA combined with the Dunnett's multiple comparison test indicated that in some cases, the relative amount of mRNA was significantly different from the wild type (denoted by *, $P < 0.001$; $n = 3$).

Figure 4: IAA6, IAA9 and IAA17 are involved in the control of adventitious root initiation

(A) Average numbers of ARs assessed in 15 *aux/iaa* knockout mutants. (B) Average numbers of ARs in *iaa6-1*, *iaa6-2*, *iaa9-1*, *iaa9-2*, *iaa17-2*, *iaa17-3* and *iaa17-6* mutant alleles. (C) Average numbers of ARs in single *iaa6-1*, *iaa9-1* and *iaa17-6* single, double and triple mutants.

(A) to (C) Seedlings were first etiolated in the dark until their hypocotyls were 6 mm long and then transferred to the light for 7 days. Data were obtained from 3 biological replicates; for each, data for at least 30 seedlings were pooled and averaged. Errors bars indicate \pm SE. In (A) and (B), one-way ANOVA combined with Dunnett's multiple comparison post-test indicated that in some cases, differences observed between the mutants and the corresponding wild type were significant (denoted by *, $P < 0.001$, $n > 30$). In (C), one-way ANOVA combined with Tukey's multiple comparison post-test indicated significant differences (denoted by different letters, $P < 0.001$, $n > 30$)

(D) to (H) Expression pattern of *IAA6*, *IAA9* and *IAA17* during the initial steps of AR formation. GUS staining of *promIAA6:GUS*, *promIAA9:GUS* and *promIAA17:GUS* (arranged from left to right in each panel) in seedlings grown in the dark until their hypocotyls were 6 mm long (D), after additional 48 h (E) and 72 h (G) after in the dark, and 48 h (F) and 72 h (H) after their transfer to the light. Bars = 5 mm.

Figure 5: IAA6, IAA9 and IAA17 repressor proteins physically interact with ARF6 and/or ARF8, while ARF6 interacts with itself to form a homodimer

(A) to (E) Co-immunoprecipitation (CoIP) assay. Arabidopsis protoplasts were transfected with a HA₃-tagged version of *IAA6*, *IAA9* or *IAA17* constructs and/or a c-Myc₃-tagged version of *ARF6* or *ARF8* constructs. Proteins were immunoprecipitated with anti-Myc antibodies and submitted to anti-cMyc protein (lower panel) to confirm the presence of the ARF protein and to anti-HA gel-blot analysis to reveal the IAA partner (top panel). HA₃-IAA6-cMyc-ARF6 (A), HA₃-IAA6-cMyc-ARF8 (B), HA₃-IAA9-cMyc-ARF8 (C), HA₃-IAA17-cMyc-ARF6 (D), HA₃-IAA17-cMyc-ARF6 (E).

(F) to (H) Arabidopsis protoplasts were transfected with HA₃-tagged and c-Myc₃-tagged versions of *ARF6* and/or *ARF8*. Proteins were immunoprecipitated with anti-HA antibodies and submitted to anti-HA protein (top panel) to confirm the presence of the ARF protein and to anti-cMyc antibody to reveal the ARF6 or ARF8 partner (lower panel). Only ARF6 homodimer could be detected (F).

(I) to (P) Confirmation of the interaction by bimolecular fluorescence complementation experiments (BiFC). Only Arabidopsis mesophyll protoplasts with intact plasma membranes, shown with bright-field light microscopy (left photo in each panel), tested positive for the presence of yellow fluorescence, indicating protein-protein interaction due to assembly of the split YFP, shown by confocal microscopy (right photo in each panel). (I) Cotransformation of 10 µg nEYFP-IAA6 and 10 µg ARF6-cEYFP into protoplasts generated yellow fluorescence (false-colored green) at the nucleus surrounded by chloroplast autofluorescence (false-colored red). Fluorescence was also observed after cotransformation of 10 µg of nEYFP-IAA6 and cEYFP-ARF8 (J); nEYFP-IAA9 and cEYFP-ARF8 (K); nEYFP-IAA17 and cEYFP-ARF6 (L); nEYFP-IAA17 and cEYFP-ARF8 (M), and nEYFP-ARF6 and cEYFP-ARF6 (N). No fluorescence was detected after cotransformation of 10 µg of nEYFP-ARF6 and cEYFP-ARF8 (O) or nEYFP-ARF8 and cEYFP-ARF8 (P). Bars = 10 µm.

Figure 6: ARF6, ARF8 and ARF17 are unstable proteins whose degradation is proteasome dependent

(A) to (D) Degradation kinetics of ARF6, ARF8 and ARF17 proteins. Top panel: representative anti-HA or anti-c-Myc western blot performed on total protein from wild-type Col-0 protoplasts transformed with 5 µg of plasmid DNA expressing HA₃- or cMyc₃- tagged proteins and mock treated with DMSO (-) or treated with 200 µg/ml of cycloheximide. Lower panel: Amido Black staining of the membrane indicating protein loading.

(E) Effect of MG132 on the degradation of the tagged ARF proteins in protoplasts. Top panel: representative anti-HA western blot performed on total protein from wild-type Col-0 protoplasts transformed with 5 µg of plasmid DNA expressing HA₃- or cMyc₃- ARF6, ARF8 and ARF17 or 15 µg of plasmid DNA expressing HA₃-ARF1 treated with MG132 (+) or mock treated with DMSO (-) for 2 h. Lower panel: Amido Black staining of the membrane indicating protein loading.

(F) Effect of MG132 on the degradation of the tagged ARF proteins *in Planta*. Top panel: representative western blot performed on total protein extracted from 7-day-old seedlings expressing HA₃-ARF1, Myc₃-ARF6, Myc₃-ARF8 or Myc₃-ARF17 treated with MG132 (+) or mock treated with DMSO (-) for 2 h. Lower panel: Amido Black staining of the membrane indicating protein loading.

ImageJ (<https://imagej.nih.gov/ij/>) was used for densitometry imaging to analyze intensity of western blot bands. The ARFs staining intensities were quantified with the area of the major pic of each cMyc- or HA-tagged versions of the proteins (above 100kDa) and divided by the density of the corresponding major loading protein. Relative target protein accumulation at t0 for the CHX treatment (A,B,C and D) or no MG132 (E and F) was set to 1 and then compared across all lanes, to assess changes across samples and ARFs stability.

Figure 7: *TIR1/AFB2-Aux/IAA6/9/17-ARF6/8* and *ARF17* signaling module is involved in the control of adventitious root initiation upstream of *GH3.3*, *GH3.5* and *GH3.6*

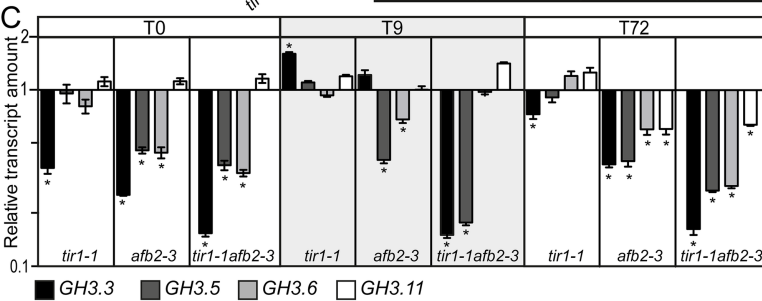
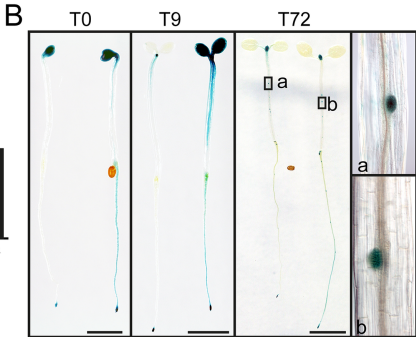
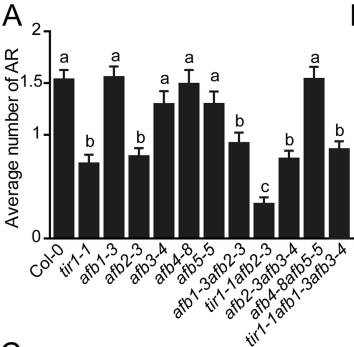
(A) Relative transcript amount of *GH3.3*, *GH3.5*, *GH3.6*, *GH3.10* and *GH3.11* genes in hypocotyls of *iaa4-1*, *iaa6-1*, *iaa9-1* and *iaa17-6* single mutants.

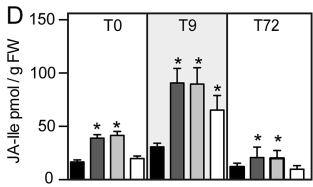
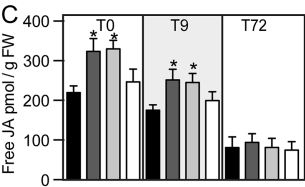
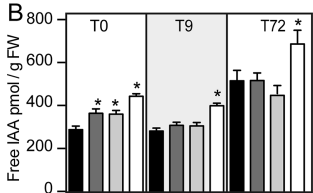
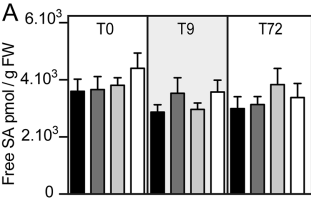
(B) Relative transcript amount of *IAA6*, *IAA9* and *IAA17* genes in hypocotyls of *iaa4-1*, *iaa6-1*, *iaa9-1* and *iaa17-6* single mutants.

In (A) and (B), mRNAs were extracted from hypocotyls of seedlings grown in the dark until the hypocotyl reached 6 mm and then transferred to the light for 72 h. Gene expression values are relative to expression in the wild type, for which the value was set to 1. The scale is a log10 scale, the extremum and minimum of each graph have been optimized according to the expression values. Error bars indicate ± SE obtained from three independent biological replicates. One-way ANOVA combined with Dunnett's multiple comparison test indicated that in some cases, the relative amount of mRNA was significantly different from the wild type

(C) Adventitious root initiation is controlled by a subtle balance of ARF activators and repressor acting upstream of JA signaling (Gutierrez et al., 2012). Under steady-state

conditions there is a balance between the positive regulators ARF6 and ARF8 and the negative regulator ARF17. The three ARFs are regulated at the transcriptional and post-transcriptional levels (Gutierrez et al., 2009) and their proteasome-dependent degradation possibly contributes to maintain their balance. IAA6, IAA9 and IAA17 protein repress the transcriptional activity of ARF6 and ARF8. The negative regulator ARF17 either interacts with ARF6 and/or ARF8 to inhibit their transcriptional activity or competes for the AuxRE elements in the promoters of the *GH3* genes. TIR1 protein controls JA biosynthesis through a pathway yet to be identified. (D) When the auxin content increases the Aux/IAA proteins form an auxin coreceptor complex with TIR1 and/or AFB2 and are sent for degradation through the 26S proteasome. In this case, the transcriptional activity of ARF6 and ARF8 is released. Therefore, the balance is shifted towards the positive regulators and results in the induction of *GH3* gene expression. The negative effect of TIR1 on JA biosynthesis is accentuated. The increased conjugation of JA by the three GH3 enzymes combined to the downregulation of JA biosynthesis will reduce the JA pool and subsequently downregulate JA signaling, resulting in increased AR initiation.

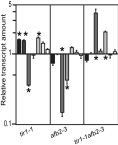




Col-0 *tir1-1* *afb2-3* *tir1-1afb2-3*

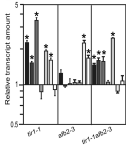
A

T0



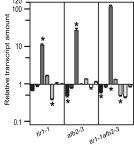
B

T9



C

T72



OPC1 OPR3 LOR2 AOC1 AOC2 AOC3 AOC4

